Chem
Europ
European C
Societies P
Check for
updates

❚ NMR Spectroscopy | *Hot Paper* |

Fast Acquisition of Proton-Detected HETCOR Solid-State NMR Spectra of Quadrupolar Nuclei and Rapid Measurement of NH Bond Lengths by Frequency Selective HMQC and RESPDOR Pulse Sequences**

Anuradha V. Wijesekara[+], [a, b] Amrit Venkatesh[+], [a, b] Bryan J. Lampkin,[a] Brett VanVeller,[a] Joseph W. Lubach,*[c] Karthik Nagapudi,*[c] Ivan Hung,[d] Peter L. Gor'kov,[d] Zhehong Gan,[d] and Aaron J. Rossini*[a, b]

Abstract: Fast magic-angle spinning (MAS), frequency selective (FS) heteronuclear multiple quantum coherence (HMQC) experiments which function in an analogous manner to solution SOFAST HMQC NMR experiments, are demonstrated. Fast MAS enables efficient FS excitation of ^{1}H solid-state NMR signals. Selective excitation and observation preserves ^{1}H magnetization, leading to a significant shortening of the optimal inter-scan delay. Dipolar and scalar ^{1}H{^{14}N} FS HMQC solid-state NMR experiments routinely provide 4- to 9-fold reductions in experiment times as compared to conventional ^{1}H{^{14}N} HMQC solid-state NMR experiments. ^{1}H{^{14}N} FS resonance-echo saturation-pulse double-resonance (RESPDOR)

allowed dipolar dephasing curves to be obtained in minutes, enabling the rapid determination of NH dipolar coupling constants and internuclear distances. ^{1}H{^{14}N} FS RESPDOR was used to assign multicomponent active pharmaceutical ingredients (APIs) as salts or cocrystals. FS HMQC also provided enhanced sensitivity for ^{1}H{^{17}O} and ^{1}H{^{35}Cl} HMQC experiments on ^{17}O-labeled Fmoc-alanine and histidine hydrochloride monohydrate, respectively. FS HMQC and FS RESPDOR experiments will provide access to valuable structural constraints from materials that are challenging to study due to unfavorable relaxation times or dilution of the nuclei of interest.

Introduction

^{14}N is an attractive nucleus for solid-state NMR spectroscopy because it has a 99.6% natural isotopic abundance. Unfortunately, ^{14}N is a spin-1 quadrupolar nucleus with a low gyromagnetic ratio (γ) and low Larmor frequency ($\nu_0 = 28.9$ MHz at

[a] A. V. Wijesekara,[+] A. Venkatesh,[+] B. J. Lampkin, Prof. B. VanVeller, Prof. A. J. Rossini
Department of Chemistry, Iowa State University, Ames, IA, 50011 (USA)
E-mail: arossini@iastate.edu

[b] A. V. Wijesekara,[+] A. Venkatesh,[+] Prof. A. J. Rossini
US DOE Ames Laboratory, Ames, IA, 50011 (USA)
E-mail: arossini@iastate.edu

[c] Dr. J. W. Lubach, Dr. K. Nagapudi
Genentech Inc., South San Francisco, CA, 94080 (USA)
E-mail: lubach.joseph@gene.com
       nagapudi.karthik@gene.com

[d] Dr. I. Hung, Dr. P. L. Gor'kov, Dr. Z. Gan
Center of Interdisciplinary Magnetic Resonance (CIMAR)
National High Magnetic Field Laboratory (NHMFL)
Tallahassee, FL, 32310 (USA)

[+] These authors contributed equally to this work.

[**] HETCOR: heteronuclear correlation; HMQC: heteronuclear multiple quantum coherence; RESPDOR: resonance-echo saturation-pulse double-resonance RESPDOR.

📄 Supporting information and the ORCID identification number(s) for the author(s) of this article can be found under:
https://doi.org/10.1002/chem.202000390.

9.4 T). Static and MAS ^{14}N solid-state NMR spectra typically cover spectral widths of several MHz because of broadening by the quadrupolar interaction.[1] Schurko and co-workers have demonstrated a number of wideline techniques for broadband signal excitation that enable routine acquisition of ^{14}N solid-state NMR spectra of stationary powders.[2] However, these experiments require ca. 50–100 mg of material and samples containing multiple ^{14}N environments may be difficult to study because overlap of ^{14}N powder patterns will complicate analysis.

Gan and Bodenhausen demonstrated that 2D heteronuclear multiple quantum coherence (HMQC) experiments can be used to indirectly detect ^{14}N signals via high-resolution magic angle spinning (MAS) ^{13}C or ^{1}H NMR signals.[3] Efficient excitation of the ^{14}N spins can be achieved with low power ^{14}N pulses or DANTE pulse trains.[3a, 4] Detection of the "spy-nucleus" simultaneously enhances sensitivity and spectral resolution.[3] Solid-state ^{1}H{^{14}N} HMQC experiments are normally performed with fast MAS frequencies above 30 kHz to enhance ^{1}H resolution and sensitivity.[4a, 5] In dipolar-HMQC (D-HMQC) experiments dipolar recoupling is applied to the spin-1/2 spy-nucleus to accelerate coherence transfer and allow observation of through-space proximities.[4a, 6] Alternative indirect detection schemes utilizing ^{1}H–^{14}N cross-polarization[7] or TRAPDOR HMQC pulse sequences using long-duration ^{14}N pulses for simultaneous recoupling and excitation have also been demonstrated.[8] Nishiyama showed that 80 kHz MAS 2D ^{1}H{^{14}N} J- or

Chemistry–A European Journal

Full Paper
doi.org/10.1002/chem.202000390

Chemistry Europe
European Chemical
Societies Publishing

D-HMQC NMR spectra of simple organic molecules such as glycine or alanine could be obtained in several minutes from less than 1 mg of material.[9] Brown and co-workers have used 60 kHz MAS ^{1}H{^{14}N} D-HMQC experiments to determine the protonation states of multicomponent active pharmaceutical ingredients (APIs).[10] They have also studied hydrogen bonding in amorphous dispersions of APIs[11] and other organic solids.[12] HMQC pulse sequences have also been applied for proton detection of half-integer quadrupolar nuclei such as ^{27}Al, ^{35}Cl, and ^{71}Ga,[13] spin-1/2 nuclei such as ^{195}Pt that exhibit large chemical shift anisotropy (CSA),[13c, 14] and low-γ spin-1/2 nuclei such as ^{89}Y.[15]

However, the intrinsically poor sensitivity of NMR spectroscopy often leads to long experiment times or prevents NMR experiments altogether. One way to improve NMR sensitivity is to use refocusing pulses, spin-locking and/or frequency-selective (FS) excitation to conserve magnetization and reduce recycle delays.[16] For example, solution ^{1}H{^{15}N} SOFAST HMQC NMR experiments on biomolecules use FS ^{1}H pulses to selectively excite and refocus high frequency amide ^{1}H NMR signals correlated to amide ^{15}N spins.[16d, e] The magnetization of ^{1}H spins in the amino acid side chains are unaffected by the FS pulses, consequently, amide ^{1}H spins are rapidly re-polarized by ^{1}H spin diffusion driven by the Overhauser effect, resulting in dramatically faster signal build-up.[16c–e] Typically, SOFAST HMQC provides 2–3 fold improved sensitivity for solution NMR experiments and order of magnitude reductions in experiment times.[16d, e]

Herein, we demonstrate that DANTE pulse trains[17] provide efficient FS ^{1}H excitation pulses for fast MAS ^{1}H solid-state NMR experiments on organic solids, enabling FS scalar or dipolar ^{1}H{^{14}N} HMQC experiments (FS J-HMQC and FS D-HMQC, respectively). The solid-state FS HMQC sequences operate in a similar manner to solution SOFAST HMQC sequences by preserving longitudinal ^{1}H magnetization that is not correlated to the heteronuclear spins of interest. FS HMQC signal build-up rates may be accelerated by a factor 4–9 compared to conventional solid-state ^{1}H{^{14}N} J- and D-HMQC, enabling application of these NMR experiments to challenging samples and previously inaccessible systems. Additionally, ^{1}H{^{14}N} FS RESPDOR experiments[18] allow rapid measurements of ^{1}H–^{14}N dipolar couplings and NH bond lengths. Accelerated acquisition of 2D ^{1}H{^{17}O} and ^{1}H{^{35}Cl} solid-state NMR spectra with FS HMQC pulse sequences is also demonstrated.

Results and Discussion

DANTE pulse trains, Gaussian pulses or low-power rectangular pulses have previously been used for frequency selective excitation and inversion in fast MAS ^{1}H solid-state NMR experiments.[19] Here, ^{1}H{^{14}N} FS HMQC was implemented by using DANTE pulse trains[17] for efficient and selective excitation of high-frequency ^{1}H spins associated with amine and ammonium groups. The DANTE blocks consist of a periodic train of small tip angle excitation pulses.[17] The pulses were 0.1 or 0.2 μs in duration (2° or 5.0° tip angle) and separated by two rotor cycles. The total duration of DANTE pulse trains was between

640 μs and 695 μs (see Supporting Information for details). The ^{1}H solid-state NMR spectrum of histidine·HCl·H$_2$O (**hist**) obtained with 50 kHz MAS shows that the amine and ammonium ^{1}H spins resonate at 17.2 ppm (H$_a$), 12.7 ppm (H$_b$), and 8 ppm (H$_c$) (Figure 1 A). Figure 1 B demonstrates that a DANTE train can selectively excite the H$_a$ ^{1}H NMR signal with 86 % efficiency of the rectangular high-power pulse. Figure 1 C shows a ^{1}H spin echo spectrum obtained with a DANTE train applied to the H$_a$ ^{1}H NMR signal prior to the broadband read pulses. This experiment demonstrates that the DANTE train minimally perturbs lower-frequency ^{1}H magnetization. I$_a$ is 0.45 in Figure 1 C, but is expected to be 0.14 because the peak intensities in Figure 1 B and 1 C should add up to 1.00. The intensity of I$_a$ is likely higher than expected in Figure 1 C because ^{1}H spin diffusion occurs during the course of the 640 μs DANTE block. In summary Figures 1 A–C show that after selective excitation of the H$_a$ ^{1}H NMR signal with a DANTE train, there is a large amount of ^{1}H magnetization that remains on the low-frequency ^{1}H spins. The high-frequency H$_a$ ^{1}H spins can then be rapidly re-polarized via ^{1}H spin diffusion.
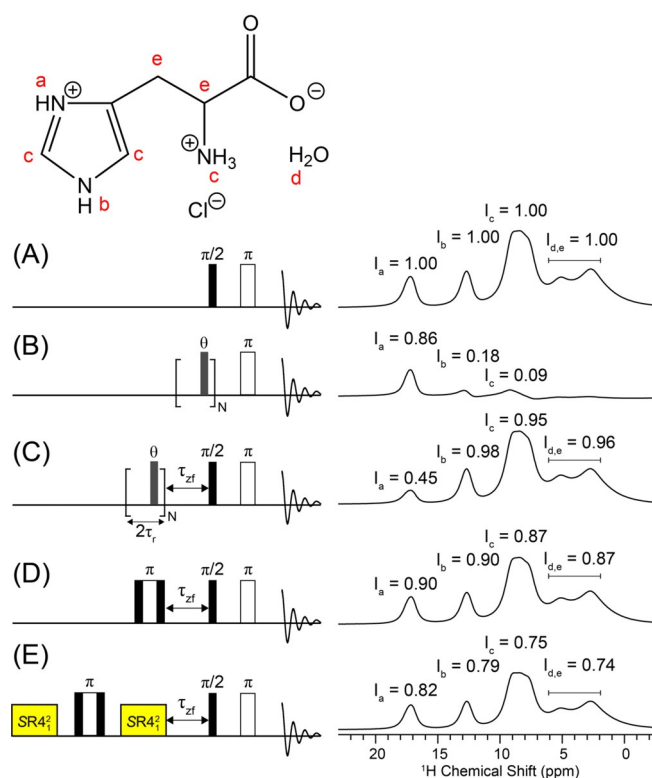
Figure 1. Quantification of DANTE excitation efficiency and magnetization losses on **hist** for pulse sequence elements required to implement solid-state FS HMQC. The molecular structure of **hist** is shown with assignment of the ^{1}H peaks. Pulse sequences are shown on the left and the resulting NMR spectra on the right. Relative ^{1}H NMR signal intensities are indicated. (A) Reference broadband spin echo spectrum. (B) Spin echo with a DANTE train for selective excitation of the highest-frequency ^{1}H NMR signal of H$_a$. (C) Selective saturation of the H$_a$ ^{1}H NMR signal with a DANTE train. (D) A broadband spin echo with a composite π -inversion pulse prior to excitation. (E) Broadband spin echo with a total of 480 μs of $SR4_1^2$ dipolar recoupling and an inversion pulse prior to excitation. All spectra were obtained with 8 scans, $\tau_{zf} = 40$ μs, $\nu_{rot} = 50$ kHz, $B_0 = 9.4$ T and inter-scan delays of 16 s (which exceed $5 \times T_1$).

Chemistry–A European Journal

Full Paper
doi.org/10.1002/chem.202000390

Chemistry Europe
European Chemical
Societies Publishing

Figure 1 D and 1 E show how to implement the remaining pulse sequence elements required for solid-state FS HMQC pulse sequences. In the solution SOFAST HMQC pulse sequence the central π-pulse must also be frequency-selective, otherwise magnetization of ^{1}H spins that were not excited by the initial π/2-pulse will be inverted, then undergo inversion recovery. However, given the short homogeneous transverse relaxation times (T_2') of ^{1}H in the solid-state it is difficult to incorporate an efficient FS-refocusing pulse into the HMQC block. Fortunately, there is a simpler solution. The magnetization of all ^{1}H spins can be inverted at the start of the sequence by a composite π-pulse (90$_Y$-180$_X$-90$_Y$, Figure 1 D and Figure 2 B). The composite pulse is more tolerant to rf inhomogeneity, slightly improving inversion efficiency.[20] The inversion pulse results in the loss of ca. 10–13 % of the ^{1}H magnetization (Figure 1 D). In the FS HMQC pulse sequence (Figure 2 B), the inversion pulse is followed by a DANTE train, then scalar or dipolar couplings evolve to generate multiple quantum coher-

ences. The broadband π-pulse then returns the longitudinal ^{1}H magnetization back to the $+z$-axis. After signal detection, the high-frequency ^{1}H spins are then repolarized by ^{1}H spin diffusion from lower-frequency ^{1}H spins, leading to shortened optimal recycle delays. Therefore, it is straightforward to implement pulse sequences analogous to SOFAST HMQC for solid-state ^{1}H{^{14}N} J-HMQC experiments where no dipolar recoupling is applied.

What about D-HMQC pulse sequences where recoupling pulse sequences are applied on the ^{1}H channel? The most widely applied recoupling sequence for proton detected D-HMQC is currently $SR4_{1'}^{2}$,[19a] which consists of an even number of π-pulses and each π-pulse has 180° phase alternation.[19a] Therefore, there will be no net rotation of longitudinal ^{1}H magnetization by $SR4_1^2$ recoupling, even in the presence of an inhomogeneous RF-field. Fortunately, longitudinal ^{1}H magnetization also decays slowly under $SR4_1^2$ symmetry-based recoupling so that there are minimal losses in longitudinal ^{1}H magnetization,
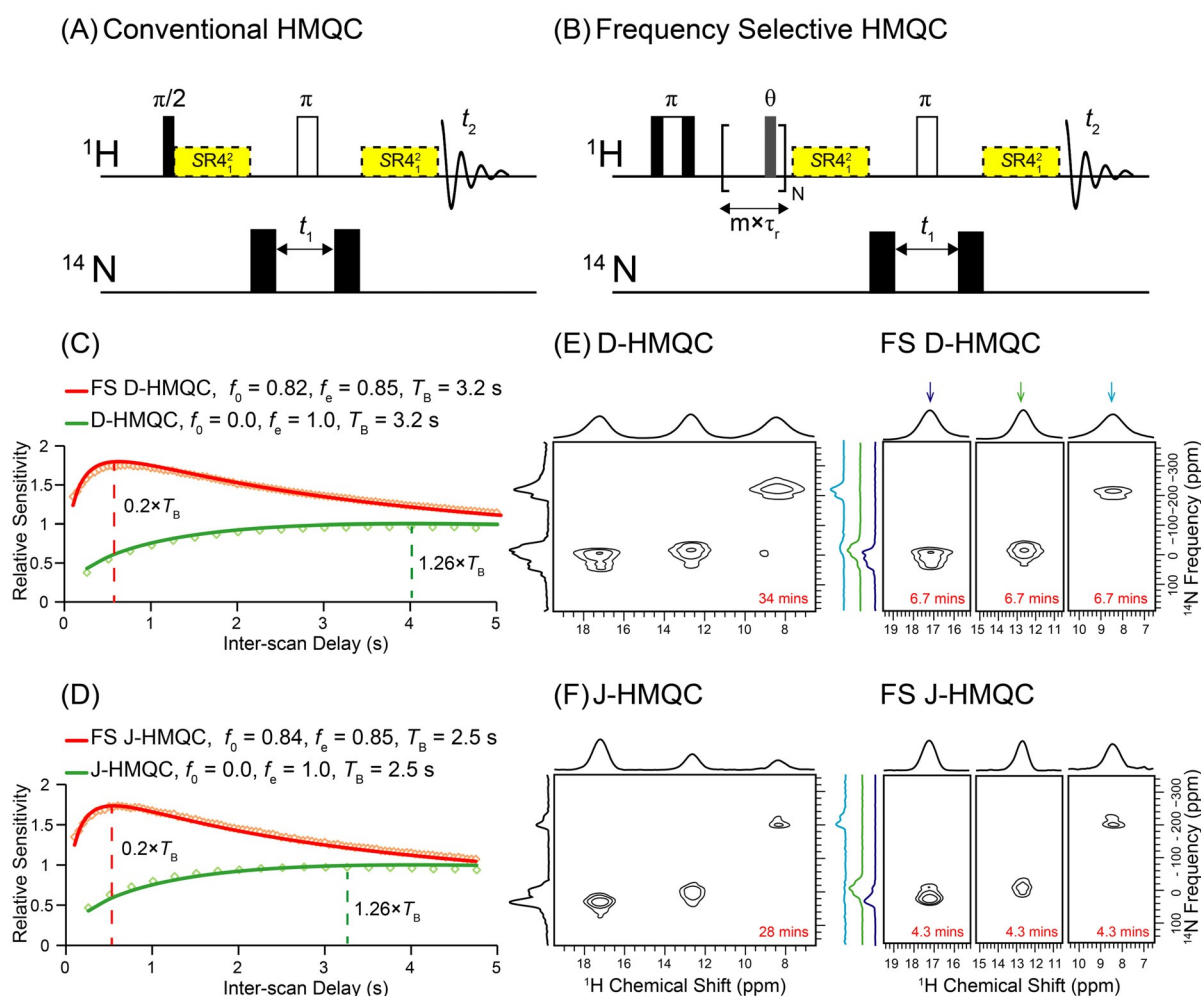
Figure 2. (A, B) Pulse sequences for (A) conventional HMQC and (B) FS HMQC. $SR4_1^2$ dipolar recoupling is not applied in the J-HMQC experiments. (C, D) Measurement of relative sensitivity for conventional and FS (C) D-HMQC and (D) J-HMQC for the H$_A$ NMR signal of **hist**. In (C) and (D) spin echo pulse sequences were used as described in the main text and Supporting Information. Experimental sensitivity curves (open diamonds) and fits to equation 1 (solid lines) are shown for the 17.2 ppm ^{1}H NMR signal. Fit parameters are indicated. (E, F) Comparison of 2D ^{1}H{^{14}N} NMR spectra of **hist** obtained with conventional and FS (E) D-HMQC and (F) J-HMQC. The FS HMQC spectra were obtained with the DANTE pulses on resonance with the different ^{1}H NMR signals. Total experiment times are indicated. D-HMQC experiments were performed with $\nu_{rot} = 50$ kHz and J-HMQC with $\nu_{rot} = 60$ kHz. All experiments performed with $B_0 = 9.4$ T.

Chemistry–A European Journal

Full Paper
doi.org/10.1002/chem.202000390

Chemistry Europe
European Chemical
Societies Publishing

even after several milliseconds of dipolar recoupling (Figure 1E and Figure S1). Overall, Figure 1 clearly illustrates that ca. 75–80% of the longitudinal ^1H magnetization can be preserved in the presence of all pulse sequence elements required for FS D-HMQC/FS RESPDOR sequences.

Scalar and dipolar $^1H\{^{14}N\}$ FS HMQC solid-state NMR experiments were performed on **hist** and compared to standard HMQC experiments (Figure 2A and 2B). Figure 2C shows measurements of the relative sensitivity (S_{rel} = signal intensity × $\tau_{rd}^{-1/2}$) as function of the inter-scan delay (τ_{rd}). FS and broadband dipole recoupled spin echo and standard spin echo pulse sequences were used for all of the relaxation experiments presented here (Figure S2). These spin echo sequences are identical to the corresponding D-HMQC/J-HMQC pulse sequences, except the ^{14}N pulses are excluded. The spin echo experiments have the same signal build-up characteristics as HMQC experiments, but offer better sensitivity for the relaxation measurements since the direct ^1H magnetization is monitored without any ^{14}N filtering/dephasing. The sensitivity curves in Figures 2C and 2D were fit with a slightly modified version of the function describing the relative sensitivity of flip-back CPMAS experiments proposed by Emsley and co-workers [Eq. (1)]:[16j]

$$S_{rel} = \frac{f_e A}{\sqrt{\tau_{rd}}} \frac{\left[1 - \exp\left(\frac{-\tau_{rd}}{T_B}\right)\right]}{\left[1 - f_0 \exp\left(\frac{-\tau_{rd}}{T_B}\right)\right]} \quad (1)$$

S_{rel} is the relative sensitivity, f_e is the efficiency of the excitation pulse, f_0 is the fraction of magnetization left after a single scan, T_B is the build-up time constant (usually equal to T_1), and A is a scaling factor adjusted so that $S_{rel} = 1.00$ for conventional HMQC experiments performed with $\tau_{rd} = 1.26 \times T_B$. For a broadband $\pi/2$ pulse $f_e = 1.0$, while for DANTE f_e may be less than 1.0 due to relaxation losses. DANTE excitation on the H_a signal of **hist** gives $f_e \approx 0.86$ (Figure 1B).

The sensitivity curve for conventional D-HMQC can be fit with $f_0 = 0.0$ and the build-up time constant (T_B) of 3.2 s matches the ^1H T_1 measured in a normal ^1H saturation recovery experiment. As expected, the recycle delay that provides optimal sensitivity is approximately 3.9 s ($1.26 \times T_B$) for conventional D-HMQC. The shape of the sensitivity curve for FS HMQC matches those previously reported for NMR experiments such as solution SOFAST HMQC or flip-back CPMAS where residual longitudinal ^1H magnetization is preserved after each scan.[16b,d,e,g,j] The fit of the FS D-HMQC sensitivity curve yields $T_B = 3.2$ s and $f_0 = 0.82$, suggesting that 82% of the ^1H polarization is retained after each scan. The conservation of ^1H magnetization leads to a reduced optimal recycle delay of 0.7 s ($0.2 \times T_B$). The faster recycling provides a factor 1.8 improvement in relative sensitivity and reduces experiment times by a factor 3.2 for FS D-HMQC as compared to standard D-HMQC. A sensitivity gain and reduction in the optimal recycle delay was also observed for FS spin echo experiments that are analogous to FS J-HMQC (Figure 2D). T_B was reduced to 2.5 s for J-HMQC experiments performed with a 60 kHz MAS frequency because of sample heating caused by increasing the MAS frequency from 50 kHz to 60 kHz. While conventional HMQC also performs well for **hist**, the sensitivity gains provided by FS HMQC enables high-quality 2D $^1H\{^{14}N\}$ dipolar- or scalar-HMQC NMR spectra of **hist** to be recorded in only a few minutes for each ^1H peak (Figures 2E and F). The sensitivity of the NMR spectra extracted from the ^1H HMQC signal at 17.2 ppm are compared in Figure S3 and the sensitivity gains with the FS HMQC experiments are consistent with the relaxation experiments.

$^1H\{^{14}N\}$ FS D- and J-HMQC experiments on **hist** were also repeated with an ultra-fast MAS frequency of 95 kHz on an 18.8 T (800 MHz) NMR spectrometer. With these conditions, the DANTE pulses have a high excitation efficiency of 96% for the H_a ^1H NMR signal (Figure S4). As expected, the efficiency and selectivity of the DANTE pulses improves with increased MAS frequency and magnetic field. One challenge with higher fields and faster MAS frequencies is that ^1H spin diffusion is slowed, which can result in a distinct ^1H T_1 for the different peaks in the spectrum,[19d,21] hindering recovery of ^1H magnetization by spin diffusion. To address this problem the conventional and the FS HMQC sequences were slightly modified for the 18.8 T experiments. The initial inversion pulse is replaced with a $90°_Y$—spin-lock$_X$—$90°_Y$ block that inverts all magnetization. The spin-lock pulse accelerates ^1H spin diffusion and makes the ^1H magnetization more homogeneous across the entire ^1H spectrum.[19d,21b] Figure S5 shows the sensitivity curves for FS and conventional D- and J-HMQC experiments at 18.8 T. For D-HMQC the gain in sensitivity was about a factor 1.8, similar to that observed at 9.4 T. However, for J-HMQC, a factor 3 gain in sensitivity was observed at 18.8 T, corresponding to a factor 9 acceleration of the experiment (Figure S6). Comparing FS J-HMQC and FS D-HMQC at 18.8 T the large gain in sensitivity for the J-HMQC experiments likely occurs because of the better efficiency of the DANTE pulse and the absence of ^1H dipolar recoupling pulses that cause some loss of magnetization. $^1H\{^{14}N\}$ FS J-HMQC spectra of **hist** were acquired in only 30 seconds each (Figure 3). The MAS spectrum of the $I = 1$ nuclei ^{14}N and ^2H are very sensitive to the precision of the magic angle setting.[1a,22] Therefore, $^1H\{^{14}N\}$ FS HMQC experiments can also be used to rapidly calibrate the magic-angle (Figure 3A). This approach is useful because when probes are configured for ^{14}N experiments there are few standards available to accurately calibrate the magic angle.

The added sensitivity and significantly reduced experiment times provided by FS HMQC are very beneficial for $^1H\{^{14}N\}$ HMQC experiments on larger molecules where NH functional groups will be more dilute. For example, multicomponent active pharmaceutical ingredients are typically formed by reacting a basic API with an acid co-former.[10,11,23] It is important to determine whether the reaction of the API and co-former results in a salt, formed when a basic group of the API is protonated, or a cocrystal, formed when the proton from the acid is not fully transferred, but forms a hydrogen bond with the API.[10,11,23] Brown and co-workers have used $^1H\{^{14}N\}$ D-HMQC[10,11] and $^{15}N\{^1H\}$ J-resolved solid-state NMR experiments[10] to qualitatively probe NH bond lengths and differentiate salts and cocrystals. Recently we have used DNP-enhanced

Chemistry–A European Journal

Full Paper
doi.org/10.1002/chem.202000390

Chemistry Europe
European Chemical
Societies Publishing
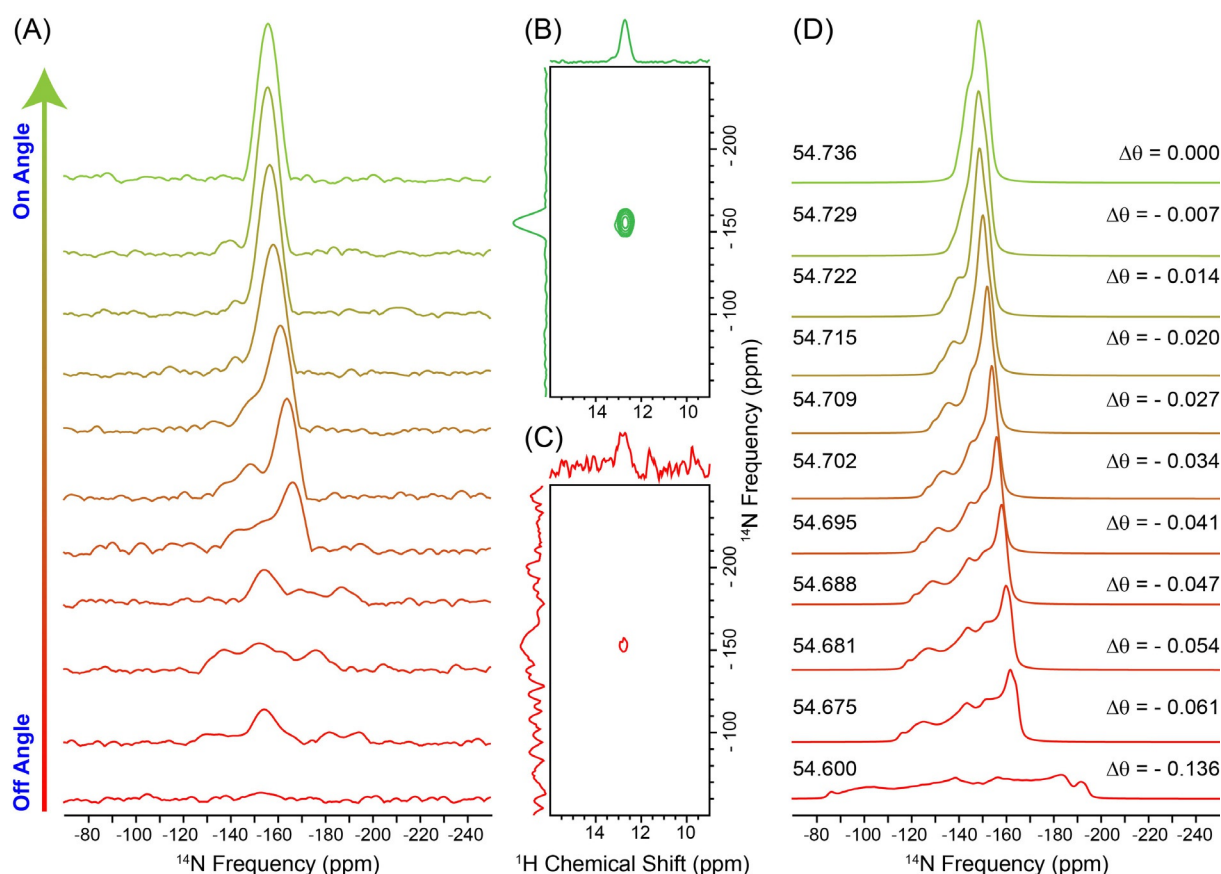
Figure 3. Setting the magic angle using FS J-HMQC and **hist**. (A) Stack of ^{14}N SSNMR spectra of **hist** extracted from 2D ^{1}H{^{14}N} FS J-HMQC. Each spectrum was obtained in 30 seconds. The upper row shows the spectrum when the magic angle is accurately adjusted and the bottom most row shows the spectrum when the magic angle is mis-set. Comparison of the 2D ^{1}H{^{14}N} FS J-HMQC spectra when (B) magic angle is accurately adjusted and (C) magic angle is mis set. All experiments were performed with $\nu_{rot} = 95$ kHz and $B_0 = 18.8$ T. (D) Analytical simulations of ^{14}N solid-state NMR spectra as a function of the MAS rotation angle with $C_Q = 1.25$ MHz and $\eta_Q = 0.7$.

^{15}N solid-state NMR to measure NH bond lengths and determine protonation states of the API GDC-0022 when it is reacted with different acid co-formers.[23]

Figure 4A shows the single-crystal X-ray diffraction structures of the tosylic acid salt of GDC-0022 (denoted as **1**) and a cocrystal formed by reacting two equivalents of GDC-0022 with fumaric acid (**2**, see Scheme S1 in the Supporting Information for full molecular structures).[23] All H-atom positions were optimized by plane-wave DFT.[23] **1** is a salt since the hydrogen atom from tosylic acid is transferred to the API ($r_{NH\ calcd} = 1.07$ Å), while **2** is a cocrystal since the hydrogen remains bound to fumaric acid and forms a hydrogen bond to the API ($r_{NH\ calcd} = 1.53$ Å and 1.55 Å, the second hydrogen bond is not shown).[23] The ^{1}H spin echo spectra of **1** and **2** shows that the hydrogen atoms involved in bonds to the API/acid co-formers resonate at high-frequency and are well resolved from the other ^{1}H NMR signals (Figure 4B), consistent with previously published DNP-enhanced 2D ^{1}H-^{15}N and ^{1}H-^{13}C HETCOR NMR spectra.[23] Note that the ^{1}H NMR signals of ammonium, amine and carboxylic groups often resonate at a high ^{1}H chemical shifts and are usually resolved from other ^{1}H NMR signals when fast MAS is used.[19d] Conventional ^{1}H{^{14}N} D-HMQC spectra of **1** and **2** recorded with short dipolar recoupling times

($\tau_{rec} < 0.75$ ms) only show the high-frequency acid ^{1}H NMR signals because these ^{1}H spins reside within 2 Å of a nitrogen atom. Consequently, FS and conventional ^{1}H{^{14}N} D-HMQC spectra of **1** and **2** will provide the exact same information, but, FS D-HMQC provides 2.2- and 1.9-fold higher sensitivity for **1** and **2**, respectively (Figures S7 and S8). The 2D ^{1}H{^{14}N} D-HMQC spectra of **1** and **2** clearly shows correlations between the ^{1}H and ^{14}N of the nitrogen and hydrogen atoms that are bonded and hydrogen bonded, respectively (Figure 4B).

^{1}H{^{14}N} HMQC and RESPDOR experiments[18] can be used to probe NH bond length and differentiate salts and cocrystals. First, the ^{14}N quadrupolar coupling constant [$C_Q(^{14}$N)] is larger for **2** than **1** as indicated by the more positive frequency of the ^{14}N SSNMR signal in **2**; the peak position is determined by the combined effects of the chemical shift and quadrupole induced shift (QIS),[3b,8b] with the latter dominating at 9.4 T. Analytically simulated ^{14}N solid-state NMR spectra are shown as dashed lines and allow $C_Q(^{14}$N) and $\delta_{iso}(^{14}$N) to be estimated (Figure 4C). The values of $C_Q(^{14}$N) and $\delta_{iso}(^{14}$N) determined from simulations in good agreement with those predicted by plane-wave DFT for **1** and **2** (Tables S1 and S2). The observed and DFT predicted differences in $C_Q(^{14}$N) for **1** and **2** suggest that $C_Q(^{14}$N) increases as the NH bond length increases. Second, NH

Chemistry–A European Journal

Full Paper
doi.org/10.1002/chem.202000390

Chemistry
Europe
European Chemical
Societies Publishing
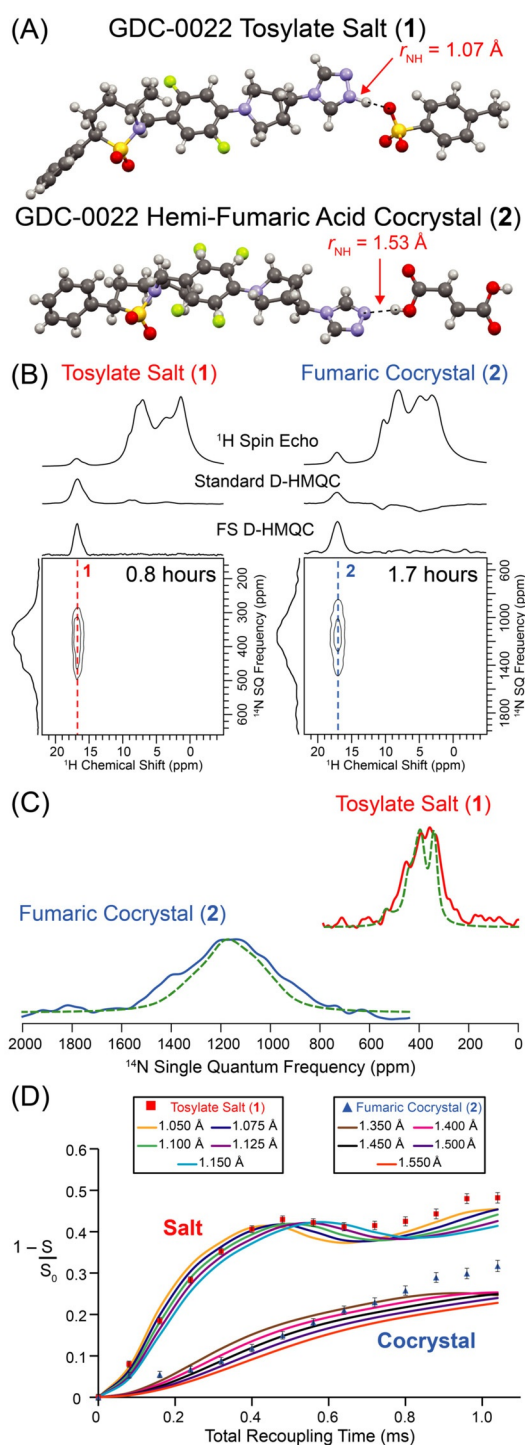
Figure 4. (A) Crystal structures of the tosylate salt (1) and hemi-fumaric acid cocrystal (2) of GDC-0022 with plane-wave DFT optimized NH bond lengths indicated. (B) ^{1}H and ^{1}H{^{14}N} D-HMQC SSNMR spectra of 1 and 2. (C) Comparison of ^{14}N SSNMR spectra of 1 and 2 and analytically simulated ^{14}N SSNMR spectra. (D) Comparison of experimental and SIMPSON simulated (solid lines) ^{1}H{^{14}N} RESPDOR dipolar dephasing curves for 1 and 2 with ^{1}H–^{14}N dipolar coupling constants corresponding to the indicated inter-nuclear distances. All experiments performed with $B_0 = 9.4$ T at $\nu_{rot} = 50$ kHz.

bond lengths can be directly measured with ^{1}H{^{14}N} RESPDOR experiments as was recently demonstrated by Nishiyama and Goldbourt.[24] However, experiment times on the order of 6–

10 hours have been reported to record ^{1}H{^{14}N} RESPDOR dipolar dephasing curves of amino acids[24] and multicomponent APIs.[25] ^{1}H{^{14}N} FS RESPDOR allowed complete dipolar dephasing curves to be obtained in only 20 minutes each for 1 and 2 (Figure 4D, Figures S9 and S10). ^{1}H{^{14}N} RESPDOR curves for 1 and 2 were calculated with the SIMPSON simulation program for a ^{1}H-^{14}N-^{14}N spin system. This 3-spin system was used to mimic the interactions present in 1 and 2. C_Q values and nitrogen chemical shifts obtained from plane-wave DFT were used in the simulations. Dipolar dephasing curves were then calculated for different dipolar coupling constants (NH bond lengths) and $r_{NH} = 1.10$ Å and $r_{NH} = 1.40$ Å were found to give the best fits for 1 and 2, respectively (Figure S9 and Figure S10). These bond lengths are in good agreement with the NH bond lengths predicted by plane-wave DFT calculations and previously measured by DNP-enhanced ^{1}H-^{15}N DIPSHIFT experiments on 1 and 2.[23] Note that the DNP-enhanced DIPSHIFT experiments required ca. 4 hours each; therefore, the ^{1}H{^{14}N} FS RESPDOR is likely the fastest and most sensitive method to measure NH bond lengths for natural abundance materials. For 2 there is substantial uncertainty in r_{NH} because the saturation factor (f) was also included as an adjustable parameter in the fits of experimental RESPDOR curves (see the Supporting Information). The accuracy of the NH bond length measurements can be improved by using a phase modulated saturation pulse to more reliably saturate the ^{14}N spins.[24, 25]

^{1}H{^{14}N} FS RESPDOR was also performed on the ammonium ^{1}H signal of **hist** at 17.2 ppm to confirm the accuracy of the NH distance measurements (Figure S11). Using ^{1}H{^{14}N} FS RESPDOR $r_{NH} = 1.10$ Å was determined, in good agreement with the value of $r_{NH} = 1.09$ Å measured by Levitt and co-workers with ^{15}N{^{1}H} symmetry-based recoupling, separated local field (SLF) experiments on ^{15}N-enriched **hist**.[26]

FS HMQC experiments were also performed on other samples and with different NMR-active nuclei. Sulfathiazole is a well-studied pharmaceutical compound with many different known polymorphs.[27] Solid-state NMR experiments on sulfathiazole are challenging because $T_1(^1$H) is very long, approximately 900 s for the sample examined here (Figure S12). Therefore, performing conventional ^{1}H{^{14}N} HMQC is extremely time consuming because inter-scan delays of ca. 1200 s would be required for optimal sensitivity and total experiment times on the order of days would result. With FS D-HMQC the inter-scan delay could be significantly reduced to ca. $0.1 \times T_1$ and a ^{1}H{^{14}N} FS D-HMQC spectrum was obtained in 8.5 hours (Figure S12). This example demonstrates FS HMQC may provide large absolute time savings for solids with long proton T_1.

Proton detected X→^{1}H D-RINEPT experiments have previously been used to obtain 2D ^{1}H-X correlation NMR spectra with X = ^{17}O and ^{35}Cl.[13b, 28] D-HMQC can theoretically provide better sensitivity than D-RINEPT because the initial polarization is derived from ^{1}H spins in the HMQC experiment, while in a D-RINEPT experiment it is derived from the lower-γ quadrupolar spin.[13b] Carboxylic acid groups often give rise to high-frequency ^{1}H NMR signals.[19d, 28a] The acid ^{1}H NMR signals can be used for ^{1}H{^{17}O} FS HMQC experiments on ^{17}O-labelled carboxylic acids. Figure 5D and E compares the conventional and FS

Chemistry–A European Journal

Full Paper
doi.org/10.1002/chem.202000390

**Chemistry
Europe**
European Chemical
Societies Publishing
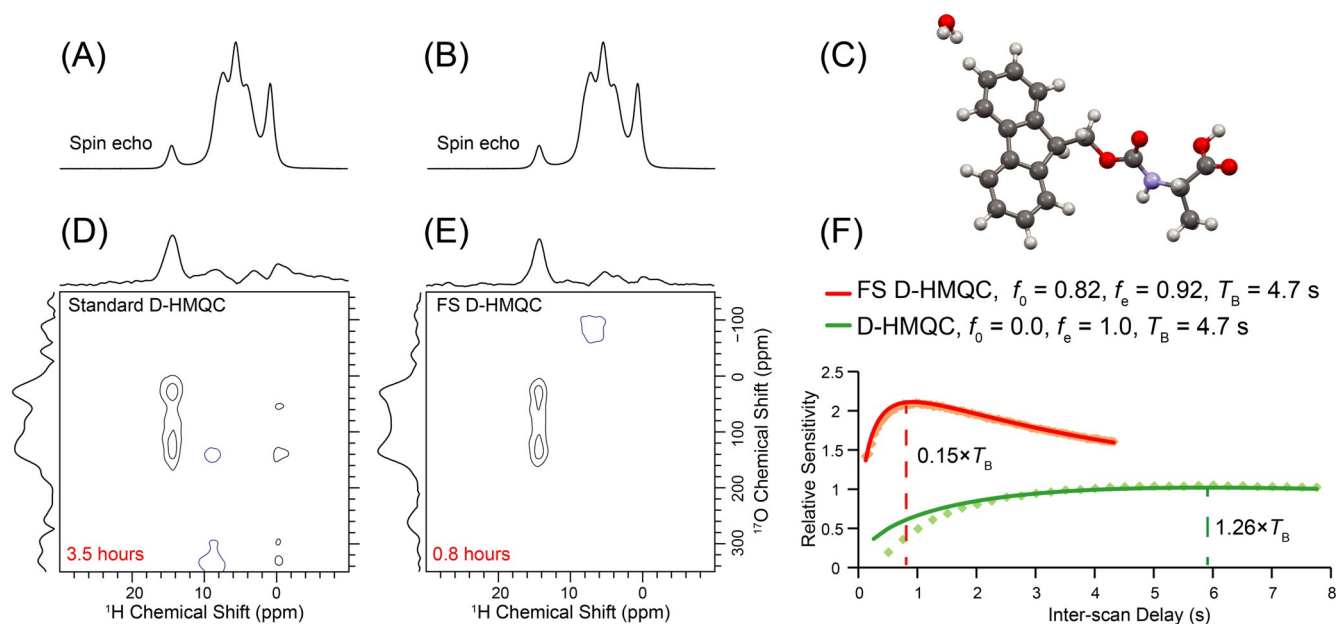
Figure 5. (A, B) ^1H spin echo NMR spectrum and (C) geometry optimized crystal structure of Fmoc-alanine. Comparison of $^1H\{^{17}O\}$ D-HMQC spectra of Fmoc-alanine obtained with (D) conventional and (E) FS pulse sequences. The experiment times for the 2D NMR spectra are indicated. (F) Measurement of the relative sensitivities for conventional and FS D-HMQC for different inter-scan delays. The fit parameters are indicated along with the curves. The experiments were performed with $B_0 = 9.4$ T at $\nu_{rot} = 50$ kHz.

$^1H\{^{17}O\}$ D-HMQC spectra of Fmoc-alanine with each oxygen atom in the carboxylic acid enriched to ca. 20% ^{17}O.[28a] Similar to the $^1H\{^{14}N\}$ HMQC experiments, a factor of 2 gain in sensitivity can be obtained for $^1H\{^{17}O\}$ FS HMQC experiments (Figure 5F), allowing a complete 2D spectrum to be obtained in only 0.8 hours. The 2D D-HMQC spectra were obtained with 80 μs of total recoupling, hence, only the ^{17}O central-transition NMR signal from the protonated oxygen atom of the carboxylic acid was observed. We previously showed that the ^1H-^{17}O J-coupling in Fmoc-alanine was 58 Hz.[28a] This J-coupling is large enough to perform $^1H\{^{17}O\}$ J-HMQC experiments (Figure S13). FS J-HMQC was two times more sensitive and four times faster than conventional J-HMQC.

^{35}Cl solid-state NMR has been shown to be a sensitive probe of molecular structure for hydrochloride salts of pharmaceuticals.[29] A $^1H\{^{35}Cl\}$ FS D-HMQC spectrum of **hist** was acquired in only 8.5 minutes (Figure S14). However, for the ^{35}Cl NMR experiments on **hist**, FS D-HMQC shows only ca. 1.3 times better sensitivity than conventional D-HMQC. The sensitivity gains are limited in the $^1H\{^{35}Cl\}$ FS HMQC experiments because the NH_3^+ groups found in the middle of the ^1H NMR spectrum show the strongest correlation to ^{35}Cl. The imperfect selectivity of the ^1H DANTE pulse trains leads to partial saturation of other ^1H spins, reducing the amount of preserved ^1H polarization and the FS HMQC sensitivity gains.

Conclusions

In summary, scalar and dipolar $^1H\{^{14}N\}$ FS HMQC solid-state NMR experiments, analogous to solution SOFAST HMQC NMR experiments, are straightforward to implement with fast MAS and can routinely provide factor 2 to 9 reductions in experiment times as compared to conventional HMQC solid-state NMR experiments. $^1H\{^{14}N\}$ FS RESPDOR experiments allowed NH internuclear distances to be rapidly determined, enabling multicomponent APIs to be assigned as salts and cocrystals. FS pulse sequences also accelerated $^1H\{^{17}O\}$ and $^1H\{^{35}Cl\}$ HMQC solid-state NMR experiments. The only criteria for FS HMQC and FS RESPDOR experiments to succeed is that the ^1H spins correlated to the hetero-nucleus are resolved from the other ^1H NMR signals. Therefore, FS HMQC and RESPDOR should be applicable to many other nuclei and these experiments should provide access to valuable structural constraints in a variety of organic, inorganic and biological systems. We also anticipate that significant time savings could also be realized with FS versions of TRAPDOR-HMQC[8a,c] and ^{14}N overtone HMQC.[30] The reduced recycle delays provided by FS experiments also allows more scans to be obtained in a given unit time which should help to reduce t_1-noise in 2D NMR experiments.[31] Finally, fast MAS is crucial to enhance ^1H NMR resolution and sensitivity and allow efficient FS excitation. Therefore, the continued development of MAS probes capable of faster MAS frequencies will likely further improve the sensitivity gains provided by the FS pulse sequences.

[1] a) H. J. Jakobsen, H. Bildsøe, J. Skibsted, T. Giavani, *J. Am. Chem. Soc.* **2001**, *123*, 5098–5099; b) L. A. O'Dell, R. W. Schurko, K. J. Harris, J. Autschbach, C. I. Ratcliffe, *J. Am. Chem. Soc.* **2011**, *133*, 527–546.

[2] a) K. J. Harris, S. L. Veinberg, C. R. Mireault, A. Lupulescu, L. Frydman, R. W. Schurko, *Chem. Eur. J.* **2013**, *19*, 16469–16475; b) L. A. O'Dell, R. W. Schurko, *J. Am. Chem. Soc.* **2009**, *131*, 6658–6659; c) R. W. Schurko, *Acc. Chem. Res.* **2013**, *46*, 1985–1995.

[3] a) S. Cavadini, A. Lupulescu, S. Antonijevic, G. Bodenhausen, *J. Am. Chem. Soc.* **2006**, *128*, 7706–7707; b) Z. H. Gan, *J. Am. Chem. Soc.* **2006**, *128*, 6040–6041.

[4] a) S. Cavadini, A. Abraham, G. Bodenhausen, *Chem. Phys. Lett.* **2007**, *445*, 1–5; b) A. G. M. Rankin, J. Trébosc, P. Paluch, O. Lafon, J.-P. Amoureux, *J. Magn. Reson.* **2019**, *303*, 28–41.

[5] a) Y. Ishii, R. Tycko, *J. Magn. Reson.* **2000**, *142*, 199–204; b) Y. Nishiyama, *Solid State Nucl. Magn. Reson.* **2016**, *78*, 24–36; c) R. Zhang, K. H. Mroue, A. Ramamoorthy, *Acc. Chem. Res.* **2017**, *50*, 1105–1113.

[6] Z. H. Gan, *J. Magn. Reson.* **2007**, *184*, 39–43.

[7] D. Carnevale, X. Ji, G. Bodenhausen, *J. Chem. Phys.* **2017**, *147*, 184201.

[8] a) J. A. Jarvis, I. M. Haies, P. T. F. Williamson, M. Carravetta, *Phys. Chem. Chem. Phys.* **2013**, *15*, 7613–7620; b) J. A. Jarvis, M. Concistre, I. M. Haies, R. W. Bounds, I. Kuprov, M. Carravetta, P. T. F. Williamson, *Phys. Chem. Chem. Phys.* **2019**, *21*, 5941–5949; c) I. Hung, P. Gor'kov, Z. Gan, *J. Chem. Phys.* **2019**, *151*, 154202.

[9] Y. Nishiyama, Y. Endo, T. Nemoto, H. Utsumi, K. Yamauchi, K. Hioka, T. Asakura, *J. Magn. Reson.* **2011**, *208*, 44–48.

[10] A. S. Tatton, T. N. Pham, F. G. Vogt, D. Iuga, A. J. Edwards, S. P. Brown, *CrystEngComm* **2012**, *14*, 2654–2659.

[11] A. S. Tatton, T. N. Pham, F. G. Vogt, D. Iuga, A. J. Edwards, S. P. Brown, *Mol. Pharm.* **2013**, *10*, 999–1007.

[12] G. N. M. Reddy, M. Malon, A. Marsh, Y. Nishiyama, S. P. Brown, *Anal. Chem.* **2016**, *88*, 11412–11419.

[13] a) M. K. Pandey, H. Kato, Y. Ishii, Y. Nishiyama, *Phys. Chem. Chem. Phys.* **2016**, *18*, 6209–6216; b) A. Venkatesh, M. P. Hanrahan, A. J. Rossini, *Solid State Nucl. Magn. Reson.* **2017**, *84*, 171–181; c) A. J. Rossini, M. P. Hanrahan, M. Thuo, *Phys. Chem. Chem. Phys.* **2016**, *18*, 25284–25295.

[14] F. A. Perras, A. Venkatesh, M. P. Hanrahan, T. W. Goh, W. Huang, A. J. Rossini, M. Pruski, *J. Magn. Reson.* **2017**, *276*, 95–102.

[15] F. A. Perras, T. W. Goh, L.-L. Wang, W. Huang, M. Pruski, *Solid State Nucl. Magn. Reson.* **2019**, *98*, 12–18.

[16] a) E. D. Becker, J. A. Feretti, T. C. Farrar, *J. Am. Chem. Soc.* **1969**, *91*, 7784–7785; b) J. Tegenfeldt, U. Haeberlen, *J. Magnetic Resonance (1969)* **1979**, *36*, 453–457; c) K. Pervushin, B. Vögeli, A. Eletsky, *J. Am. Chem. Soc.* **2002**, *124*, 12898–12902; d) P. Schanda, B. Brutscher, *J. Am. Chem. Soc.* **2005**, *127*, 8014–8015; e) P. Schanda, Ē. Kupče, B. Brutscher, *J. Biomol. NMR* **2005**, *33*, 199–211; f) J. J. Lopez, C. Kaiser, S. Asami, C. Glaubitz, *J. Am. Chem. Soc.* **2009**, *131*, 15970–15971; g) A. Lupulescu, L.

Frydman, *J. Chem. Phys.* **2011**, *135*, 134202; h) T. Gopinath, G. Veglia, *Angew. Chem. Int. Ed.* **2012**, *51*, 2731–2735; *Angew. Chem.* **2012**, *124*, 2785–2789; i) J. R. Banigan, N. J. Traaseth, *J. Phys. Chem. B* **2012**, *116*, 7138–7144; j) S. Björgvinsdóttir, B. J. Walder, A. C. Pinon, J. R. Yarava, L. Emsley, *J. Magn. Reson.* **2018**, *288*, 69–75; k) N. T. Duong, J. Trébosc, O. Lafon, J.-P. Amoureux, *Solid State Nucl. Magn. Reson.* **2019**, *100*, 52–62; l) S. Jayanthi, A. Lupulescu, *Solid State Nucl. Magn. Reson.* **2020**, *107*, 101652.

[17] a) G. Bodenhausen, R. Freeman, G. A. Morris, *J. Magn. Reson.* **1976**, *23*, 171–175; b) G. A. Morris, R. Freeman, *J. Magn. Reson.* **1978**, *29*, 433–462.

[18] a) L. Chen, Q. Wang, B. Hu, O. Lafon, J. Trébosc, F. Deng, J.-P. Amoureux, *Phys. Chem. Chem. Phys.* **2010**, *12*, 9395–9405; b) Z. H. Gan, *Chem. Commun.* **2006**, 4712–4714.

[19] a) A. Brinkmann, A. P. M. Kentgens, *J. Am. Chem. Soc.* **2006**, *128*, 14758–14759; b) V. S. Mithu, K. O. Tan, P. K. Madhu, *J. Magn. Reson.* **2013**, *237*, 11–16; c) A. J. Robertson, M. K. Pandey, A. Marsh, Y. Nishiyama, S. P. Brown, *J. Magn. Reson.* **2015**, *260*, 89–97; d) D. A. Hirsh, V. A. Wijesekara, S. L. Carnahan, I. Hung, J. W. Lubach, K. Nagapudi, A. J. Rossini, *Mol. Pharm.* **2019**, *16*, 3121–3132.

[20] M. H. Levitt, *eMagRes* **2007**, https://doi.org/10.1002/9780470034590.emrstm0086.

[21] a) Y. Q. Ye, M. Malon, C. Martineau, F. Taulelle, Y. Nishiyama, *J. Magn. Reson.* **2014**, *239*, 75–80; b) A. Venkatesh, I. Hung, K. C. Boteju, A. D. Sadow, P. L. Gor'kov, Z. Gan, A. J. Rossini, *Solid State Nucl. Magn. Reson.* **2020**, *105*, 101636.

[22] a) A. K. Khitrin, B. M. Fung, *J. Chem. Phys.* **1999**, *111*, 8963–8969; b) T. Giavani, H. Bildsøe, J. Skibsted, H. J. Jakobsen, *Chem. Phys. Lett.* **2003**, *377*, 426–432; c) S. Antonijevic, G. Bodenhausen, *Angew. Chem. Int. Ed.* **2005**, *44*, 2935–2938; *Angew. Chem.* **2005**, *117*, 2995–2998.

[23] L. Zhao, M. P. Hanrahan, P. Chakravarty, A. G. DiPasquale, L. E. Sirois, K. Nagapudi, J. W. Lubach, A. J. Rossini, *Cryst. Growth Des.* **2018**, *18*, 2588–2601.

[24] N. T. Duong, F. Rossi, M. Makrinich, A. Goldbourt, M. R. Chierotti, R. Gobetto, Y. Nishiyama, *J. Magn. Reson.* **2019**, *308*, 106559.

[25] D. Bernasconi, S. Bordignon, F. Rossi, E. Priola, C. Nervi, R. Gobetto, D. Voinovich, D. Hasa, N. T. Duong, Y. Nishiyama, M. R. Chierotti, *Cryst. Growth Des.* **2020**, *20*, 906–915.

[26] X. Zhao, J. L. Sudmeier, W. W. Bachovchin, M. H. Levitt, *J. Am. Chem. Soc.* **2001**, *123*, 11097–11098.

[27] D. C. Apperley, R. A. Fletton, R. K. Harris, R. W. Lancaster, S. Tavener, T. L. Threlfall, *J. Pharm. Sci.* **1999**, *88*, 1275–1280.

[28] a) S. L. Carnahan, B. J. Lampkin, P. Naik, M. P. Hanrahan, I. I. Slowing, B. VanVeller, G. Wu, A. J. Rossini, *J. Am. Chem. Soc.* **2019**, *141*, 441–450; b) E. G. Keeler, V. K. Michaelis, M. T. Colvin, I. Hung, P. L. Gor'kov, T. A. Cross, Z. Gan, R. G. Griffin, *J. Am. Chem. Soc.* **2017**, *139*, 17953–17963.

[29] a) H. Hamaed, J. M. Pawlowski, B. F. T. Cooper, R. Fu, S. H. Eichhorn, R. W. Schurko, *J. Am. Chem. Soc.* **2008**, *130*, 11056–11065; b) M. Hildebrand, H. Hamaed, A. M. Namespetra, J. M. Donohue, R. Q. Fu, I. Hung, Z. H. Gan, R. W. Schurko, *CrystEngComm* **2014**, *16*, 7334–7356; c) D. A. Hirsh, A. J. Rossini, L. Emsley, R. W. Schurko, *Phys. Chem. Chem. Phys.* **2016**, *18*, 25893–25904.

[30] L. A. O'Dell, R. He, J. Pandohee, *CrystEngComm* **2013**, *15*, 8657–8667.

[31] F. A. Perras, M. Pruski, *J. Magn. Reson.* **2019**, *298*, 31–34.